J|A|C|S
ARTICLES
Published on Web 02/14/2003

Decisive Role of Electronic Polarization of the Protein Environment in Determining the Absorption Maximum of Halorhodopsin

Minoru Sakurai,* Keiko Sakata, Shino Saito, Sawako Nakajima, and Yoshio Inoue

Contribution from the Department of Biomolecular Engineering, Tokyo Institute of Technology, 4259 Nagatsuta-cho, Midori-ku, Yokohama 226-8501, Japan

Received June 18, 2002; E-mail: msakurai@bio.titech.ac.jp

Abstract: It is known that the absorption maximum of halorhodopsin is red shifted by 10 nm with the uptake of a chloride ion Cl^-. According to the X-ray structure, the ion is located at the position of the counterion of the chromophore, protonated retinal Schiff base. Thus, the direction of the observed spectral change is opposite to that expected from the π-electron redistribution (an increase in the bond alternation) induced by the counterion. The physical origin of this abnormal shift is never explained in terms of any simple chemical analogues. We successfully explain this phenomenon by a QM/MM type of excitation energy calculation. The three-dimensional structure of the protein is explicitly taken into account using the X-ray structure. We reveal that the electronic polarization of the protein environment plays an essential role in tuning the absorption maximum of halorhodopsin.

Introduction

Retinal is commonly found as a chromophore in the vertebrate visual pigments such as rhodopsin[1] and in bacterial light-transducing proteins, including the proton pump bacteriorhodopsin, the chloride pump halorhodopsin, and the phototaxis pigments sensory rhodopsin I and II.[2] The chromophore is bound to the respective apoprotein via a protonated Schiff base linkage to a specific lysine residue. As a result, these proteins are able to absorb visible light, triggering the photoreactions responsible for their physiological functions. Their absorption maxima are widely distributed in the visible spectrum region,[1,2] whereas that of the free protonated retinylidene Schiff base absorbs at 440 nm in methanol.[3] A major issue in the retinal protein photochemistry is elucidating the origin of such a spectral shift, induced by transfer of the chromophore from the solution state to the protein-binding state.

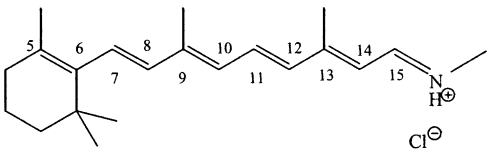

protonated *all-trans* retinylidene Schiff base

There is a long history of theoretical investigations of this spectral shift.[4] One of the key factors that has been accepted commonly would be the counterion effect. The longer (shorter) the distance between the Schiff base nitrogen and the counterion is, the longer (shorter) the absorption wavelength is. This is naturally understood considering that the increase (decrease) in the distance causes an increase (decrease) in π-electron delocalization along the conjugated chain. Undoubtedly, the protein in which the counterion is missing should absorb at a longer wavelength than does the native protein. However, the opposite phenomenon has been found in halorhodopsin (HR). A recent X-ray study of HR has indicated that Cl^- forms a salt bridge with the Schiff base as if it were a counterion.[6] Nevertheless, binding of Cl^- to the protein causes a red shift of about 10 nm (Table 1).[5,6] The elucidation of such an abnormal spectral shift is a highly challenging issue to theoreticians and is expected to shed new insight into the mechanistic role of the protein environment.

In this study, the absorption maximum of HR was calculated using the QM/MM-CI (quantum mechanics/molecular mechanics-configuration interaction) method recently developed by our group to interpret the spectral shift in bacteriorhodopsin.[4h] In this theory, the electronic polarization of the protein environ-

(1) Kochendoerfer, G. G.; Lin, S. W.; Sakmar, T. P.; Mathies, R. A. *Trends Biochem. Sci.* **1999**, *24*, 300.
(2) Oesterhelt, D. *Curr. Opin. Struct. Biol.* **1998**, *8*, 489.
(3) Blatz, P. E.; Johnson, R. H.; Mohler, J. H.; Al-Dilaimi, S. K.; Dewhurst, S.; Erickson, J. O. *Photochem. Photobiol*. **1971**, *13*, 237.
(4) (a) Honig, B.; Dinur, U.; Nakanishi, K.; Balogh-Nair, V.; Gwainowics, M. A.; Aranaboldi, M.; Motto, M. G. *J. Am. Chem. Soc*. **1979**, *101*, 7084. (b) Raudino, A.; Zuccarello, F.; Buemi, G. *J. Chem. Soc., Faraday Trans*. **1983**, *79*, 1759. (c) Kakitani, H.; Kakitani, T.; Rodman, H.; Honig, B. *Photochem. Photobiol*. **1985**, *41*, 471. (d) Luzhkov, V.; Warshel, A. *J. Am. Chem. Soc*. **1991**, *113*, 4491. (e) Beppu, Y.; Kakitani, T. *Photochem. Photobiol*. **1994**, *59*, 660. (f) Sakai, K.; Vacek, G.; Lüthi, H. P.; Nagashima, U. *Photochem. Photobiol*. **1997**, *66*, 532. (g) Houjou, H.; Inoue, Y.; Sakurai, M. *J. Am. Chem. Soc*. **1998**, *120*, 4459. (h) Houjou, H.; Inoue, Y.; Sakurai, M. *J. Phys. Chem. B* **2001**, *105*, 867. (i) Hayashi, S.; Tajkhorshid, E.; Pebay-Peyroula, E.; Royant A.; Landau, E. M.; Navarro, J.; Shulten, K. *J. Phys. Chem. B* **2001**, *105*, 10124. (j) Kusnetzow, A.; Dukkipati, A.; Babu, K. R.; Singh, D.; Vought, B. W.; Knox, B. E.; Birge, R. R. *Biochemistry* **2001**, *40*, 7832. (k) Ren, L.; Martin, C. H.; Wise, K. J.; Gillespie, N. B.; Luecke, H.; Lanyi, J. K.; Spudich, J. L.; Birge, R. R. *Biochemistry* **2001**, *40*, 13906. (l) Warshel, A.; Chu, Z. T. *J. Phys. Chem. B* **2001**, *105*, 9857. (m) Rajamani, G.; Gao, J. *J. Comput. Chem*. **2002**, *23*, 96.
(5) Kolbe, M.; Besir, H.; Essen, L.-O.; Oesterhelt, D. *Science* **2000**, *288*, 1390.
(6) Schobert, B.; Lanyi, J. K.; Oesterhelt, D. *J. Biol. Chem.* **1986**, *261*, 2690.

10.1021/ja027342k CCC: $25.00

Table 1. The Decomposition of the First $\pi \rightarrow \pi^*$ Excitation Energy and the Calculated Absorption Maxima for the Four Ion Pairs Model and the Experimental Absorption Maxima

	decomposition of the excitation energy[a] /10^{-4} au					absorption maximum /nm	
	$\Delta E'$	$\mathbf{Q}^{\mathrm{I}}\mathbf{G}\mathbf{q}^{\mathrm{II}}$	$\mathbf{q}^{\mathrm{I}}\mathbf{G}\mathbf{q}^{\mathrm{II}}$	$^1/_2\mathbf{q}^{\mathrm{II}}\mathbf{R}\mathbf{q}^{\mathrm{II}}$	$\mathbf{q}^{\mathrm{II}}\mathbf{R}\mathbf{Q}^{\mathrm{II}}$	λ_{max} (calc.)[b]	λ_{max} (exp.)[c]
Cl^--occupied	1031	−17	−72	36	−150	541	578
Cl^--unoccupied	925	51	−95	48	−64	523	565
difference[d]	106	−68	24	−12	−86	18 (−619)[e]	13 (−397)[e]

[a] $\Delta E'$ corresponds to eq 5. The other terms related to $\mathbf{q}^{\mathrm{II}}$ correspond to the second to fourth terms on the right-hand side of eq 4. As described in the text, these four terms are calculated for the HOMO → LUMO transition in the CI wave function. Thus, the sum of $\Delta E'$ and these terms is not equal to the value of the calculated absorption maximum given in the seventh column in this table. [b] Calculated absorption maximum. [c] Experimental absorption maximum taken from ref 6. [d] Difference obtained by subtracting the value in the Cl^--unoccupied state from that in the Cl^--occupied state. [e] The values in parentheses are the absorption maximum differences given in cm^{-1}.

ment, induced by excitation of the chromophore, is explicitly taken into account. It is found that a major origin of the abnormal spectral shift mentioned above is the electrostatic interactions between the Cl^- ion and the protein polarization charges. The present study is an excellent example indicating that the polarizable nature of a protein significantly contributes to the occurrence of its function.

Theory

We briefly describe the OM/MM-CI method used here. In this method, the whole protein is divided into two regions, that is, region I and region II. Region I involves the chromophore and the chloride ion and three water molecules (see Figure 4), and it is treated quantum-mechanically. Region II corresponds to the residual protein part and is approximated by classical electrostatics. It is assumed that regions I and II have the atomic charge distributions $\mathbf{Q}^{\mathrm{I}}$ and $\mathbf{Q}^{\mathrm{II}}$, respectively, in the ground state. Each component of the column vectors $\mathbf{Q}^{\mathrm{I}}$ and $\mathbf{Q}^{\mathrm{II}}$ is the net charge on each atom in the corresponding region. For example, the atomic charges of the *a*th and *m*th atoms in regions I and II are given by

$$(\mathbf{Q}^{\mathrm{I}})_a = Q_a{}^{\mathrm{I}}$$
$$(\mathbf{Q}^{\mathrm{II}})_m = Q_m{}^{\mathrm{II}} \quad (1)$$

Upon excitation of the chromophore, the charge rearrangements are induced in both regions. The vectors $\mathbf{q}^{\mathrm{I}}$ and $\mathbf{q}^{\mathrm{II}}$ represent the atomic charge rearrangements induced by the excitation in regions I and II, respectively. For example, $(\mathbf{q}^{\mathrm{I}})_a$ is the charge alteration of the *a*th atoms in region I. As a result, in the excited state, the atomic charge distributions of regions I and II become $(\mathbf{Q}^{\mathrm{I}} + \mathbf{q}^{\mathrm{I}})$ and $(\mathbf{Q}^{\mathrm{II}} + \mathbf{q}^{\mathrm{II}})$, respectively. The charge distributions of regions I and II interact with each other through an operator **G** defined as follows:

$$(\mathbf{G})_{am} = \frac{1}{|\mathbf{r}_a - \mathbf{r}_m|} \quad (2)$$

where $\mathbf{r}_a$ and $\mathbf{r}_m$ are the position vectors of atoms *a* and *m*, respectively. Similarly, to describe the electrostatic interaction inside the region II, a matrix **R** is introduced as follows:

$$(\mathbf{R})_{mn} = \frac{1}{|\mathbf{r}_m - \mathbf{r}_n|} \qquad (m \neq n)$$
$$(\mathbf{R})_{mm} = 0 \quad (3)$$

where $\mathbf{r}_m$ and $\mathbf{r}_n$ are the position vectors of atoms *m* and *n*, respectively.

In the framework of CI theory, the *i*th excitation energy ΔE_i of the whole protein is expressed as follows (eqs 19 and 20 in ref 4h):

$$\Delta E_i = \Delta E_i' + (\mathbf{Q}^{\mathrm{I}} + \mathbf{q}^{\mathrm{I},i})\mathbf{G}\mathbf{q}^{\mathrm{II},i} + \frac{1}{2}\mathbf{q}^{\mathrm{II},i}\mathbf{R}\mathbf{q}^{\mathrm{II},i} + \mathbf{q}^{\mathrm{II},i}\mathbf{R}\mathbf{Q}^{\mathrm{II}} \quad (4)$$

$$\Delta E_i' = E_i^{\mathrm{I}} - E_0{}^{\mathrm{I}} + \mathbf{q}^{\mathrm{I},i}\mathbf{G}\mathbf{Q}^{\mathrm{II}} \quad (5)$$

where E_i^{I} and $E_0{}^{\mathrm{I}}$ represent the total energies of the *i*th excited and ground states of region I in the absence of region II. Equation 5 represents the excitation energy of region I which is placed in the electrostatic field generated from the protein charge distribution $\mathbf{Q}^{\mathrm{II}}$. Hereafter the approximation based on eq 5 is called the "fixed charge model". The second to fourth terms on the right-hand side of eq 4 represent the Coulombic energy corrections due to the electronic polarization of the protein environment.

$\mathbf{Q}^{\mathrm{I}}$ and $\mathbf{q}^{\mathrm{I}}$ were obtained using a semiempirical CI method with the INDO/S parameter set,[7] and $\mathbf{Q}^{\mathrm{II}}$ was evaluated using a linear-scaling molecular orbital method[8] that can explicitly take into account all of the atoms of the protein based on the X-ray structure. $\mathbf{q}^{\mathrm{II}}$ was evaluated using our unique model called the polarizable mosaic model (PMM), where all of the covalent bonds of the protein were approximated by cylindrically shaped dielectrics with appropriate dielectric constants. The cylindrical dielectric connecting atoms *m* and *n* have a polarizability of α_{mn}, the value of which was determined from corresponding experimental data (see Table 1 of ref 4h). When an electric field is applied to the dielectric, partial charges q_m and q_n ($= -q_m$) are induced on both edges of the cylinder, resulting in an induced dipole moment μ_{mn}.

$$\mu_{mn} = q_m d_{mn} \approx -\alpha_{mn}\frac{\phi_n - \phi_m}{d_{mn}} \quad (6)$$

where d_{mn} is the bond length between atoms *m* and *n*, and ϕ_m is the electrostatic potential at the center of the atom *m*. From this equation, we can evaluate q_m because α_{mn} is known. In a general case, the following equation is deduced:

$$\mathbf{q}^{\mathrm{II}} = \mathbf{A}\Phi \quad (7)$$

(7) Rajzman, M.; Francois, P. *QCPE 11* **1979**, 382.
(8) Stewart, J. J. *Int. J. Quantum Chem.* **1996**, *58*, 133.

Matrix **A** and column vector Φ are given by

$$A_{mn} = \frac{\alpha_{mn}}{d_{mn}^2} \qquad (m \neq n) \tag{8}$$

$$A_{mn} = -\sum_n \frac{\alpha_{mn}}{d_{mn}^2} \tag{9}$$

$$(\Phi)_m = \phi_m \tag{10}$$

Because $\mathbf{q}^{II}$ is induced in response to $\mathbf{q}^{I}$, the main source of the electrostatic potential in eq 10 is the induced charges $\mathbf{q}^{I}$. In addition, $\mathbf{q}^{II}$ must be corrected for the mutual polarization among the $\mathbf{q}^{II}$ charges themselves. Thus, ϕ_m depends on the induced charges and coordinates of all of the atoms except atom *m*. Thus

$$\Phi = \mathbf{G}^t\mathbf{q}^I + \mathbf{R}\mathbf{q}^{II} \tag{11}$$

By substituting eq 11 into eq 7, we can obtain the expression of $\mathbf{q}^{II}$

$$\mathbf{q}^{II} = (\mathbf{I} - \mathbf{A}\mathbf{R})^{-1}\mathbf{A}\mathbf{G}^t\mathbf{q}^I \tag{12}$$

where **I** is the unit matrix.

Calculations

The initial atomic coordinates of HR were taken from the Protein Data Bank (the PDB entry code is 1E12). This structure includes the Cl^- ion. Hydrogen atoms were added using the Insight II program. The positions of all of the atoms except the backbone heavy atoms were optimized by the linear-scaling molecular orbital method mentioned above.[8] For the Cl^--unoccupied state, the initial structure was taken from the same X-ray data in which the Cl^- ion was deleted and the geometry optimization was carried out in the same way as above. In our study, the ionization state of the protein was assumed on the basis of the following considerations: (i) ionizable groups present in the protein interior tend to form ion pairs if they are in contact with each other, (ii) we partially referred to the results of the electrostatic calculation given by Kolbe et al.,[5] and (iii) all of the ionizable groups exposed to aqueous medium were set to be neutral. Item iii is not unreasonable, because the dielectric screening effect of the solvent cancels out the charges of the ionized residues located on the protein surface. This has been demonstrated by our recent study on the effects of hydration on the electronic structure of a protein.[9] The four ion pairs model described in the next section satisfies all of the above three items. As a result, there are four sets of ion pairs: the Schiff base−Cl^-, Arg 108−Asp 238, Arg 161−Glu 219, and Asp 197−Arg 200.

Results and Discussion

Electronic Structure of the Chromophore in HR. First, we compare the charge distributions along the polyene chain of the chromophore between the ground and first $\pi-\pi^*$ excited states. The results are shown in Figures 1 and 2, where the solid and dashed lines represent the data for the Cl^--occupied and -unoccupied states, respectively. These results were obtained under the fixed charge approximation given in eq 5, and thereby

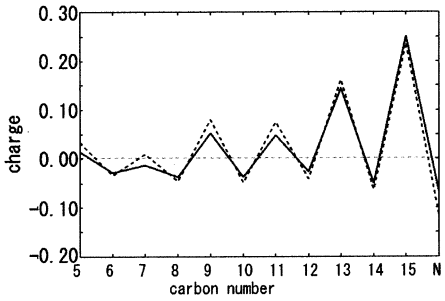

Figure 1. The net charges on the conjugated carbon and Schiff base nitrogen atoms in the ground state. The solid and dashed lines represent the data for the Cl^--occupied and -unoccupied states, respectively.

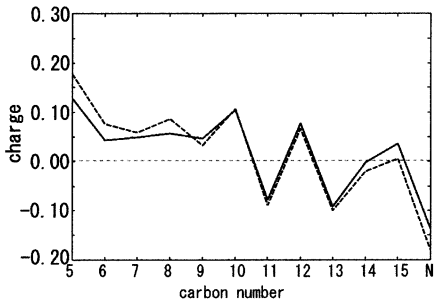

Figure 2. The net charges on the conjugated carbon and Schiff base nitrogen atoms in the first $\pi-\pi^*$ excited state. The solid and dashed lines represent the data for the Cl^--occupied and -unoccupied states, respectively.

the effect of the protein electrostatic field is explicitly taken into account. In the ground state, positive charges are distributed on the odd-numbered carbons, and the magnitudes become smaller toward the β-ionone ring (Figure 1). In contrast, in the excited state, the positive charges are largely delocalized toward the β-ionone ring, and consequently the C5−C10 atoms are positively charged. Thus, on going from the ground state to the first $\pi-\pi^*$ excited state, the positive charges move from the Schiff-base side to the β-ionone ring. Such charge transfer corresponds to $\mathbf{q}^{I}$ and occurs irrespective of whether the Cl^- ion is present or not. It is known that different charge analysis often yields very different charge distributions. To examine the validity of our semiempirical results, Figures 1 and 2 were compared with results of higher level of theory. González-Luque et al. have reported CASSCF results for the charge distributions of a truncated model compound of protonated retinal Schiff base (Figure 4 in ref 10). The data for the S_0 and S_1 states in their report correspond to Figures 1 and 2 in the present study, respectively. The present data were confirmed to be in good agreement with the CASSCF data except for the charge on the Schiff base nitrogen: in ref 10, the Schiff base nitrogen was positively charged. In ref 10, the Schiff base side is terminated by the $-C{=}NH_2^+$ group, while our model has the $-C{=}NH^+-CH_2-CH_3$ group. The different results for the nitrogen charges seem to be due to such a structural difference, because in our model the proton charge is allowed to be delocalized to the ethyl group as well. Despite the difference in the nitrogen charge, the charge rearrangement ($\mathbf{q}^{I}$) along the polyene chain, induced by excitation from S_0 to S_1, is very similar between the present result and the CASSCF one.

Next, we compare the charge distributions along the polyene chain of the chromophore between the Cl^--occupied and

(9) Ohno, K.; Kamiya, N.; Asakawa, N.; Inoue, Y.; Sakurai, M. *J. Am. Chem. Soc.* **2001**, *123*, 8161.

(10) González-Luque, R.; Garavelli, M.; Bernardi, F.; Merchán, M.; Robb, M. A.; Olivucci, M. *Proc. Natl. Acad. Sci. U.S.A.* **2000**, *97*, 9379

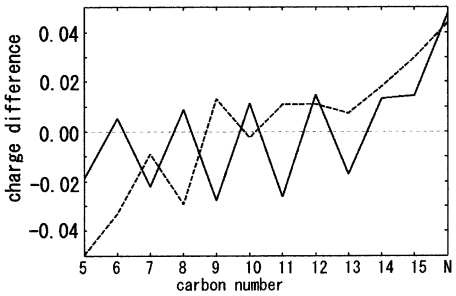

Figure 3. The charge rearrangement on the conjugated system induced by binding of the Cl^- ion. The solid and dashed lines represent the data for the ground and first $\pi-\pi^*$ excited states, respectively. The value for each atom was obtained by subtracting the net charge in the Cl^--unoccupied state from that in the Cl^--occupied state.

-unoccupied states. Figure 3 shows the charge differences obtained by subtracting the data for the Cl^--unoccupied state from those of the Cl^--occupied state, where the solid and dashed lines represent the results for the ground and excited states, respectively. In the ground state, the odd-numbered carbons from C5 to C13 have negative values, and the C14, C15, and N atoms have positive values. This clearly indicates that on going from the Cl^--unoccupied state to the Cl^--occupied state, the positive charges tend to be localized toward the Schiff base linkage. In the excited state, such a charge rearrangement is more remarkable (dashed line). These results indicate that the bond alternation of the polyene chain increases with binding of the Cl^- ion, which is consistent with the usual picture of counterion effect as described in the Introduction. Therefore, as far as we focus our attention on the chromophore electronic structure alone, its absorption maximum is expected to shift to red with binding of the Cl^- ion. However, this is inconsistent with the experimental result for HR. In other words, the consideration of the electronic states of the chromophore (region I) alone is insufficient to interpret the experimental spectral shift. The photon energy absorbed also perturbs the energy state of the protein environment (region II) surrounding the chromophore. As will be described in the next section, the polarization nature of the protein essentially contributes to causing a red shift of the absorption maximum of the whole protein.

Absorption Maximum of HR. Table 1 summarizes the results for the excitation energy calculation together with the experimental absorption maxima of HR. The seventh column of this table indicates the calculated absorption maxima (given in nm) for the Cl^--occupied and -unoccupied states. Each value corresponds to the total excitation energy ΔE in eq 4. Interestingly, on going from the Cl^--unoccupied to -occupied states, the absorption maximum shifts to red by 18 nm, which is in fairly good agreement with the experimental data (13 nm).

To examine the mechanism of the red shift, the excitation energy was decomposed according to the scheme given in eq 4. Here this decomposition scheme was applied only to the HOMO $\rightarrow$ LUMO contribution in the CI expansion, because it is difficult to pick up each of the second to fourth terms in eq 4 from the whole CI wave function. Our CI calculation indicated that the CI coefficient of the HOMO $\rightarrow$ LUMO transition was 0.959, which means that the first $\pi \rightarrow \pi^*$ excitation energy is dominated by this transition. Therefore, the above approximate treatment is reasonable to examine the relative contributions of the five terms on the right-hand side of eq 4. Obviously, the terms $\mathbf{Q^I G q^{II}}$ and $\mathbf{q^{II} R Q^{II}}$ are decisively responsible for the red shift. The former represents the Coulombic interaction between the ground-state charge distribution in region I and the induced charge distribution $\mathbf{q^{II}}$ in region II, and the latter represents the interaction between the ground-state charge distribution in region II and the induced charges $\mathbf{q^{II}}$ in itself. Among the two terms, the former's physical meaning can be easily visualized as shown in Figure 4, where the electrostatic potentials generated from $\mathbf{q^{II}}$ are plotted on the plane including the retinal conjugated system and on a plane perpendicular to the conjugated plane. As can be seen, the protein environment in the vicinity of the protonated Schiff base linkage exhibits positive potentials (blue), and that on the β-ionone side exhibits negative potentials (orange). A similar electrostatic potential map was also obtained for the Cl^--unoccupied state (data not shown). The occurrence of such a characteristic polarization can be easily explained if we take into account the characteristic charge transfer caused by excitation of the chromophore. As described in the previous section, the proton on the Schiff base is delocalized toward the β-ionone ring on going from the ground to the first $\pi-\pi^*$ excited state. In response to this charge transfer in region I, the protein environment is polarized so as to cancel out the electric field change generated in region I. Consequently, the polarization charge distribution $\mathbf{q^{II}}$, giving the potential profile shown in Figure 4, appears in the excited state. Interestingly, Figure 4

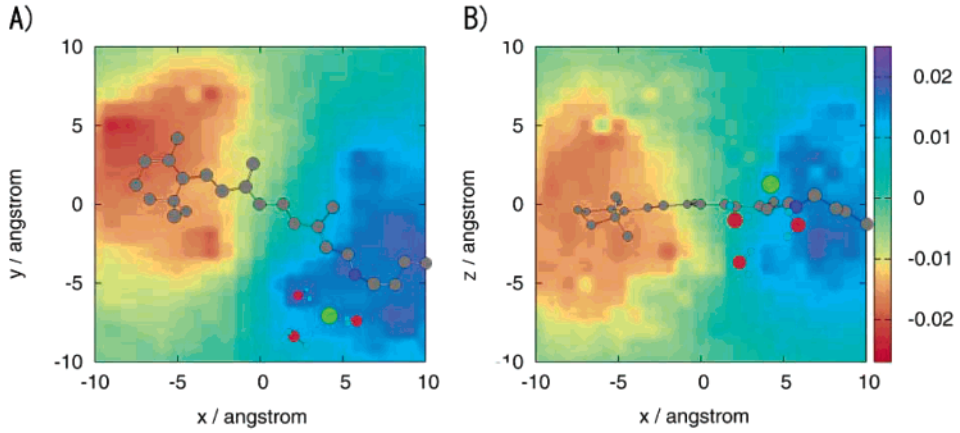

Figure 4. The electrostatic potential map made by $\mathbf{q^{II}}$. The retinylidene Schiff base, chloride ion (green circle), and three nearby water molecules were included in region I. (A) Map drawn on the conjugated plane, (B) map drawn on the plane perpendicular to the conjugated plane and involving C10 and C11 atoms. The unit of color scale is au.

Table 2. The Decomposition of the First $\pi \rightarrow \pi^*$ Excitation Energy and the Calculated Absorption Maxima for the Two Ion Pairs Model and the Experimental Absorption Maxima

	decomposition of the excitation energy[a] /10^{-4} au					absorption maximum /nm	
	$\Delta E'$	$\mathbf{Q}^{\mathrm{I}}\mathbf{G}\mathbf{q}^{\mathrm{II}}$	$\mathbf{q}^{\mathrm{I}}\mathbf{G}\mathbf{q}^{\mathrm{II}}$	$1/2\mathbf{q}^{\mathrm{II}}\mathbf{R}\mathbf{q}^{\mathrm{II}}$	$\mathbf{q}^{\mathrm{II}}\mathbf{R}\mathbf{Q}^{\mathrm{II}}$	λ_{max} (calc.)[b]	λ_{max} (exp.)[c]
Cl^--occupied	1005	−21	−88	44	−121	548	578
Cl^--unoccupied	924	50	−96	48	−58	522	565
difference [d]	81	−71	8	−4	−63	26 (−915)[e]	13 (−397)[e]

[a] See footnote *a* of Table 1. [b] Calculated absorption maximum. [c] Experimental absorption maximum taken from ref 6. [d] Difference obtained by subtracting the value in the Cl^--unoccupied state from that in the Cl^--occupied state. [e] The values in parentheses are the absorption maximum differences given in cm^{-1}.

reveals that the Cl^- ion is put in a positive potential region. Therefore, in the excited state of the Cl^--occupied protein, an additional attractive interaction between the Cl^- ion and the positive potential from $\mathbf{q}^{\mathrm{II}}$ is caused through the term $\mathbf{Q}^{\mathbf{I}}\mathbf{G}\mathbf{q}^{\mathbf{II}}$. As a result, the value of $\mathbf{Q}^{\mathrm{I}}\mathbf{G}\mathbf{q}^{\mathrm{II}}$ for the Cl^--occupied state is much smaller than that for the Cl^--unoccupied state (see Table 1), leading to a red shift. A similar illustrative explanation is not easy for the term $\mathbf{q}^{\mathbf{II}}\mathbf{R}\mathbf{Q}^{\mathbf{II}}$, and thus the numerical results alone are presented in the sixth column of Table 1.

To examine the dependence of the absorption maximum on the conformation and ionization states of the protein, we calculated the absorption maximum for another ionization state, where only two ion pairs, Arg 108−Asp 238 and the Schiff base−Cl^-, were formed in the protein interior. In this model, only the nearest neighbor ionizable groups around the Schiff base were ionized. Similar to the case of the four ion pairs model, we carried out geometry optimization using the linear-scaling molecular orbital method. This led to a structure with side chain conformations different from those of the four ion pairs model. The results of the excitation energy calculation are summarized in Table 2. It was again indicated that binding of Cl^- causes a red shift (26 nm in this case) and the terms $\mathbf{Q}^{\mathbf{I}}\mathbf{G}\mathbf{q}^{\mathbf{II}}$ and $\mathbf{q}^{\mathbf{II}}\mathbf{R}\mathbf{Q}^{\mathbf{II}}$ are main contributors to the red shift. In addition, the electrostatic potential maps generated from $\mathbf{q}^{\mathbf{II}}$ were very similar to Figure 4 (data not shown). Thus, it is confirmed that the mechanism of the red shift is not affected by the conformation and ionization states of the protein.

Finally, it is of interest to consider the contribution of $\Delta E'$ in eq 4. As described in the Theory section, this term involves the perturbation from the protein (fixed) atomic charges given by $\mathbf{Q}^{\mathbf{II}}$ (see eq 5). Technically, this perturbation energy is automatically calculated by introducing a perturbation term, such as $(\mathbf{G}\mathbf{Q}^{\mathrm{II}})$, into the Fock matrix (see eq 17 of ref 4h). Thus, the protein charge $\mathbf{Q}^{\mathrm{II}}$ directly modifies the electronic structure and orbital energies of the chromophore, leading to a spectral shift. As can be seen from Table 1, the difference, $\Delta E'$(occupied) − $\Delta E'$(unoccupied), is 106×10^{-4} au, corresponding to a significant blue shift. This result is quite consistent with the prediction from the electronic structure changes shown in Figure 3. Therefore, the inclusion of the fixed charge $\mathbf{Q}^{\mathbf{II}}$ alone fails to account for the experimental data. In other words, the nonpolarizable protein environment (fixed charge model) is inappropriate for reproducing the abnormal spectral shift of HR.

Conclusion

The photon energy absorbed not only excites the chromophore but also changes the electrostatic energy of the protein environment. Consequently, the absorption maximum (excitation energy) of the whole protein is determined by the synergistic effect of the chromophore excitation and the protein electrostatics. The change in the electrostatic energy of the protein part, depending on the polarization charges $\mathbf{q}^{\mathbf{II}}$, plays an essential role in tuning the absorption maximum of the whole protein. The present study is an excellent example indicating that the polarizable nature of a protein significantly contributes to the occurrence of its function and strongly supports the repeated statement by Warshel's group that the inclusion of induced dipoles is crucial for the proper calculation of physical properties of proteins.[4d,l]

Acknowledgment. The authors thank the Computer Center, Institute for Molecular Science, Okazaki, Japan, for the use of the supercomputer system. They also thank the Computer Center, Tokyo Institute of Technology, for the use of the SGI origin 2000 system. This work was supported by Grant-in-Aid No. 12680653.

JA027342K